Supplementary materials

Table S1. The match list of structurally similar proteins searched by $EnpA_{CD}$ structure query in Dali server (1-15) and manual search (16). Grey shading indicates catalytic domains of proteins for which the specific activity was demonstrated.

No:	PDB id	Dali Z score/ RMSD/%id	Protein name and origin	Hydrolytic activity
1	2GU1	18.4/ 2.3/ 29	Lysostaphin like peptidase (VC0503) from *Vibrio cholerea*	No data
2	3SLU	17.6/ 1.9/ 39	Lysostaphin like, outer membrane protein (NMB0315) from *Neisseria meningitidis*	No data
3	5J1K	16.5/ 2.3/ 28	Cell shape determinant (Csd2) from *Helicobacter pylori*	Not active - degenerated active site
4	1QWY	16.3/ 2.2/ 36	LytM glycyl-glycine hydrolase from *Staphylococcus aureus*	Active
5	4LXC	16/ 2.3/ 30	Lysostaphin glycyl-glicine hydrolase from *Staphylococcus simulans*	Active
6	2HSI	16/ 2.1/ 31	Putative M23 from *Pseudomonas aeruginosa*	No data
7	4RNY	15.9/ 2.6/ 34	Cell shape determinant (Csd3) from *Helicobacter pylori*	Active
8	5J1M	15.5/ 2.2/ 32	Cell shape determinant (Csd1) from *Helicobacter pylori*	No data
9	3TUF	15.3/ 2.4/ 29	Stage III sporulation protein from *Bacillus subtilis*	Not active - degenerated active site
10	3NYY	13.5/ 2.3/ 26	Putative M23 from *Ruminococcus gnavus*	No data
11	5GT1	12.6/ 2.2/ 21	Choline binding protein (CbpA) from *Lactobacillus salivarius str. Ren*	No data
12	3CSQ	11.8/ 2.8/ 16	Gp13 protein – lysozyme-like from bacteriophage φ29	Active
13	5KVP	11.5/ 2.7/ 32	ZoocinA endopeptidase from *Streptococcus equi subsp. Zooepidemicus*	Active
14	3IT5	10.8/ 2.7/ 22	LasA protease from *Pseudomonas aeruginosa*	Active
15	5b0h-A	10.8/ 2.8/ 17	Leukocyte cell-derived chemotaxin2 from *Homo sapiens*	Not active - degenerated active site
16	5kqb	15.4/1.9/33	LytU peptidoglycan endopeptidase from *Staphylococcus aureus*	Active

Table S2. Specificity of $EnpA_{CD}$. Bacteriolytic activity of $EnpA_{CD}$ was measured as OD_{620} decrease of bacterial suspension collected at logarithmic growth phase, suspended to OD_{620} of 1.0 in 50 mM glycine buffer pH 8.0 with or without 100mM NaCl and treated with 500nM $EnpA_{CD}$ for 1 hour. The results are presented as % of reduction of initial OD_{620} after 1 hour normalized to the control (without enzyme). All assays were run in triplicates and repeated at least twice.

Bacteria	Source	Cross-bridge connected to D-Ala-	Activity (%) ± standard deviation	
			ionic strength	
			low	high
Lactococcus lactis	CCM 1877	D-Asp	0±0	6±3
Enterococcus faecium	CCM 7167		3±3	7±4
Micrococcus luteus	ATCC 10240	L-Ala-D-Glu(Gly)-L-Lys-D-Ala	32±4	0±0
Bacillus subtilis	IBB 886	Direct	5±2	3±3
Streptococcus oralis	CCM 7412		7±3	2±1
Aerococcus viridans	CCM 1914		22±3	11±2
Streptococcus equi subsp. zooepidemicus	CCM 7316	L-Ala2-3	0±4	0±4
Streptococcus ratti	CCM 7443		9±8	7±6
Streptococcus pyogenes	CCM 7418		21±1	3±0
Streptococcus agalactiae	IBB 130		28±4	5±7
Enterococcus faecalis	IBB 421		34±10	2±4
Enterococcus faecalis	CCM 4224		38±9	3±3
Enterococcus faecalis	CCM 1875		39±10	0±0
Salinicoccus roseus	CCM 168	Gly5-6	84±2	7±9
Staphylococcus cohnii	DSM 20260		15±4	0±1
Staphylococcus xylosus	PCM 2114		16±0	0±2
Staphylococcus lugdunensis	PCM 2430		40±2	1±1
Staphylococcus agnetis	DSMZ 23656		19±3	0±3
Staphylococcus carnosus subsp. carnosus	DSM 20501		20±0	0±2
Staphylococcus aureus 8325-4	NCTC 8325		43±6	1±4
Staphylococcus saprophyticus	ATCC 15305	(L-Ser-Gly)1-2-Gly3-4	78±8	n.d.
Staphylococcus capitis	PCM 2121		14±2	0±2

Staphylococcus pasteuri	PCM 2445		15±1	0±4
Staphylococcus haemolyticus	PCM 2113		21±3	0±4
Staphylococcus intermedius	DSM 20373		22±7%	2±0%
Staphylococcus warneri	PCM 2107		29±4%	0±6%
Staphylococcus simulans	DSM 20037		87±4%	0±0%
Staphylococcus simulans	CCM 3583		65±4%	4±0%
Staphylococcus epidermidis	ATCC12228		4±1%	0±0%
Staphylococcus pettenkoferi	VCU 012		0±3%	0±0%
Staphylococcus pettenkoferi	DSM 19554		10±1%	0±0%
Staphylococcus pettenkoferi	Vesteras 18:1		51±7%	0±2%

Table S3. Summary of X-ray data collection, relevant data processing and the model refinement statistics. Values in parentheses are for the highest resolution shell.

Data collection and processing	
Beamline	P13 (DASY, Hamburg)
Wavelength (Å)	0.9116
Resolution range (Å)	47.79 - 2.99 (3.10 - 2.99)
Space group	P 6_5 2 2
Unit cell (Å, °)	136.5, 136.5, 325, 90, 90, 120
Total no. of reflections	802631 (36807)
No. of unique reflections	36798 (3579)
Multiplicity	21.9
Completeness (%)	99.84 (99.11)
Mean I/σ(I)	16.6 (1.1)
R_{meas} (%)	21.6 (299.7)
$CC_{1/2}$	99.9 (43.4)
Refinement	
Reflections in working set	34966 (3403)
Reflections in test set	1841(179)
R_{work} (%)	22.5 (39.4)
R_{free} (%)	25.9 (42.4)
Number of non-H atoms	4883
macromolecule	4839
ligands	5
water	39
RMS(bonds) (Å)	0.007
RMS(angles) (°)	0.96
Ramachandran favored (%)	94.65
Ramachandran outliers (%)	0
Rotamer outliers (%)	0
Clashscore	7.42
Average B-factor ($Å^2$)	99.6
macromolecule	99.8
ligands	85.9
water	80.8
Number of TLS groups	5

Figure S1. Crystal packing. **(A)** A sphere representation of crystal packing showing the content of the four adjacent unit cells, restricted by lines representing crystal axis labeled with lower cases. Each layer of molecules is arranged around 6_5 axis (c axis) and is depicted in distinct color. Molecules of one asymmetric unit are labelled A, B, C, D and E. **(B)** A representation of non-crystallographic 5_1 2 symmetry. Five molecules of the asymmetric unit A-E are represented by the surface and molecules related by the two-fold crystallographic symmetry A' - E' are shown as a spheres. Molecules AB, CD, EE', D'C' and B'A' create dimers internally related by non-crystallographic two-fold symmetry. **(C)** View along the 5_1 propagating axis. All dimers are paired by the line to depict non-crystallographic 5_1 symmetry perpendicular to hexagonal axis. Consecutive dimers are twisted at around 72° angle.

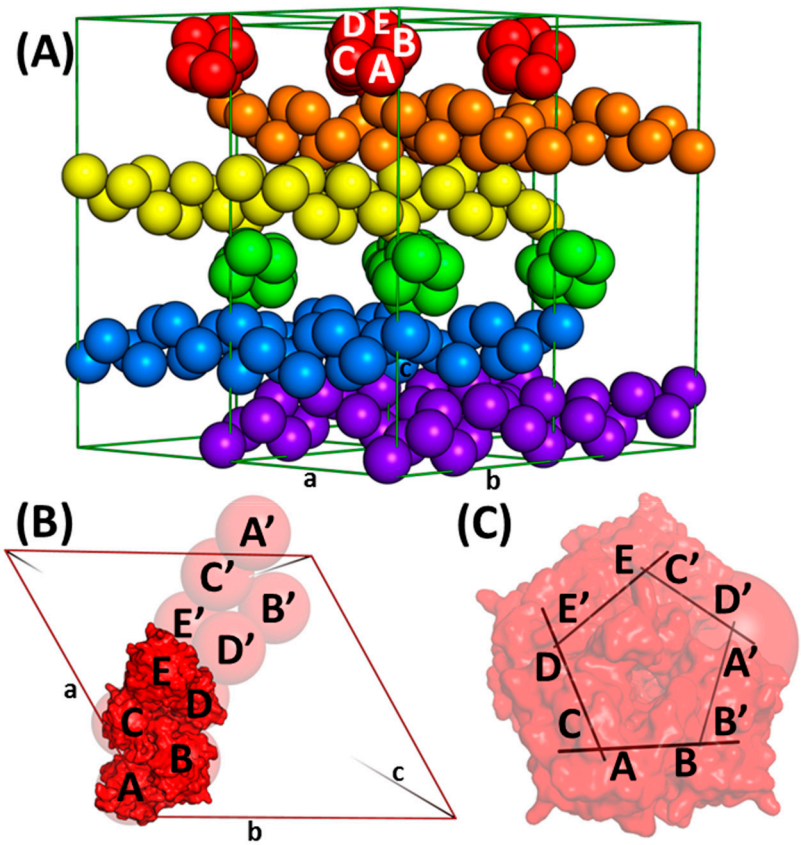

The crystal is composed of layers of molecules arranged around hexagonal axis (**Fig. 2A**). All protein molecules are packed as dimers related by non-crystallographic 2-fold symmetry. Molecules in dimers are propagating along the axis perpendicularly to six fold symmetry. Consecutive dimers rotate by approximately 72° creating a twisted coil (double helix) which implies non-crystallographic 5_1 screw axis. Together with crystallographic 2-fold axis, it creates $5_1 2$ symmetry **(Fig. 2B)**. The crystal contacts connecting separated coils are observed along the crystallographic 6_5 screw axis and it is the only joint between them **(Fig. 2C)**. Similar helical arrangement of crystalized molecules were reported previously[66].

Figure S2. Relevant amino acid residues around an active site, metal ion and water molecule shown as sticks, green sphere and red sphere respectively. The position of atoms are evidenced by the (2mFo-DFc, αc) map in black contoured at 1 σ within 2 A of selected atoms.

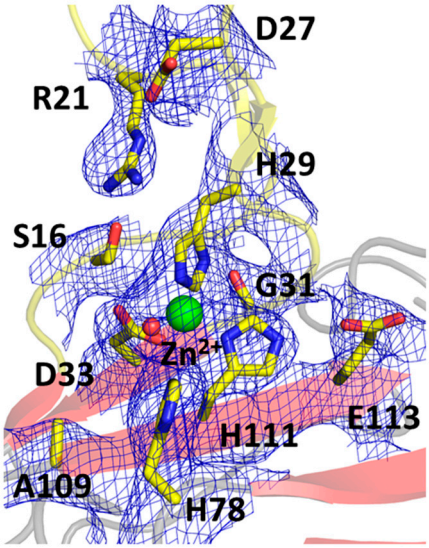

Figure S3. A spaghetti representation of superimposed catalytic domains of proteins structurally related to $EnpA_{CD}$. Constant **(A)** and variant **(B)** elements are separated. The core of $EnpA_{CD}$ on (B) is shown as red semi-transparent cartoon; an active site ion as a green sphere. Color code is used as following: $EnpA_{CD}$ - red; M23 from *Vibrio cholerae* (PDB id:2gu1)- orange; NMB0315 from *Neisseria meningitidis* (PDB id: 3slu) - grey; Csd2 from *Helicobacter pylorii* (PDB id:5j1k) - navy blue; LytM (PDB id:1qwy) - magenta; Lss (PDB id:4lxc) - cyan; M23 from *Pseudomonas aeruginosa* (PDB id:2HSI) - lime; Csd3 from *Helicobacter pylori* (PDB id:4rny) - light pink; Csd1 from *Helicobacter pylori* (PDB id:5j1m) - chocolate; channel complex from *Bacillus subtilis* (PDB id:3tuf) light blue, M23 from *Ruminococcus gnavus* (RUMGNA_02482) (PDB id:3nyy) -purple; M23 from *Lactobacillus salivarius* REN (PDB id:5gt1) - black; bacteriophage Φ29 (PDB id:3csq) - green; ZoocinA from *Streptococcus equi* (PDB id:5kvp) - yellow; LasA from *Pseudomonas aeruginosa* (PDB id:3it5) – deep olive; Chemotaxin2 from human leukocyte (PDB id:5B0H) - white; LytU from a *Staphylococcus aureus* (PDB id:KQB) - marine.

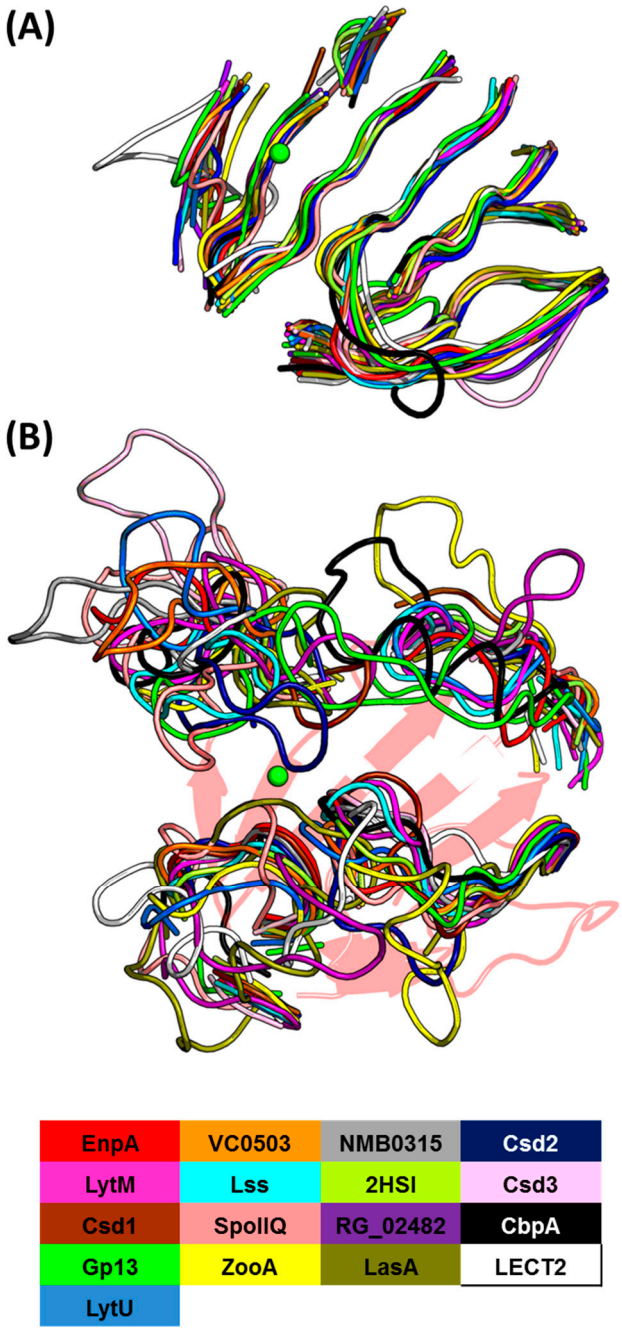

Figure S4. Dependence of ionic strength and buffer composition on $EnpA_{CD}$ activity . Showed as results of the lytic test (turbidity reduction assay) carried out on *S. aureus* 8325-4 strain in 50mM glycine buffer pH = 8.0. The enzyme concentration is indicated and each bar represents the mean of three measurements.

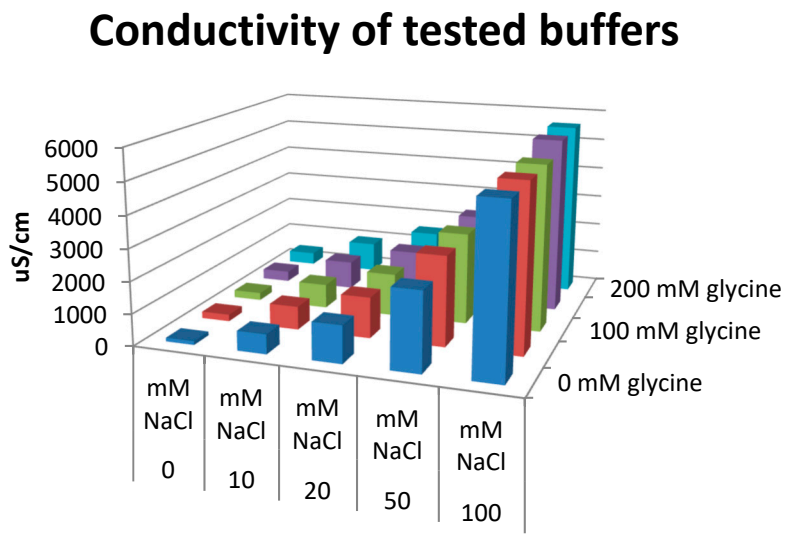

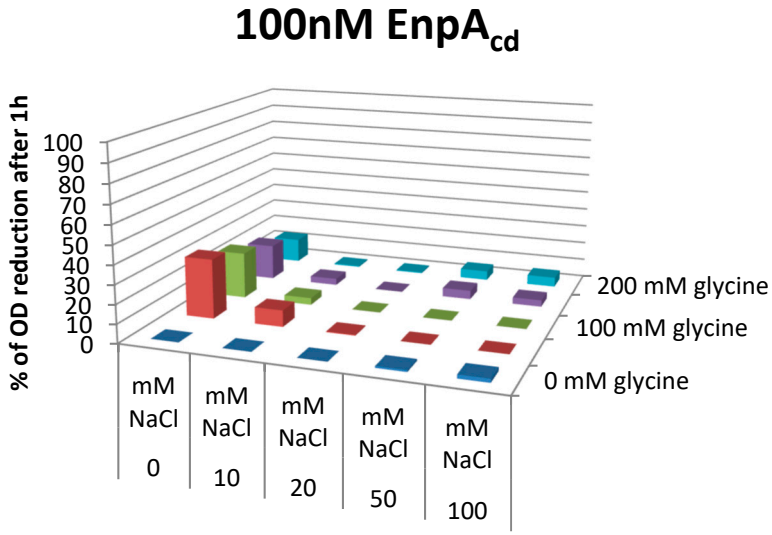

500nM $EnpA_{cd}$

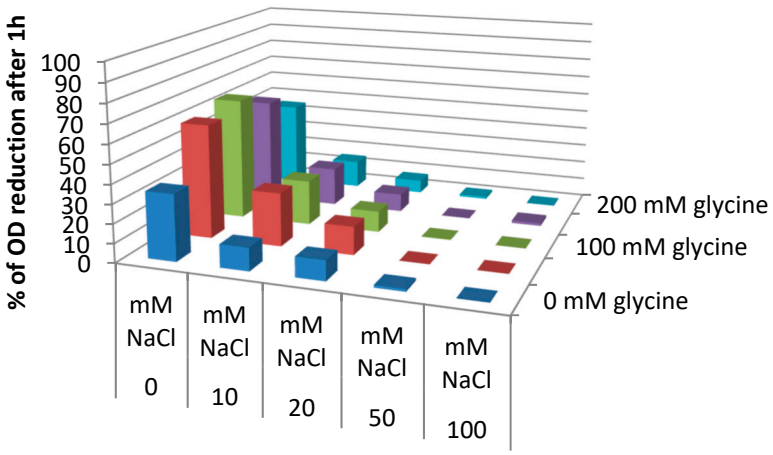

1000nM $EnpA_{cd}$

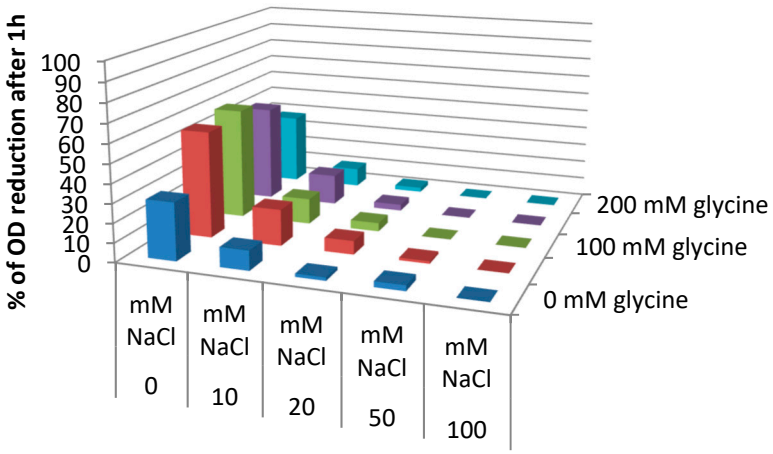

2000nM $EnpA_{cd}$

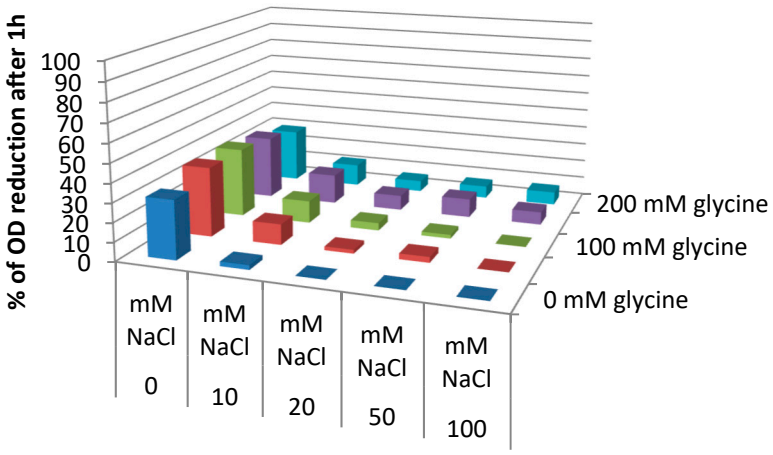

Figure S5. The effect of temperature on $EnpA_{CD}$ activity against *S. aureus* 8325-4. Activity was measured using turbidity reduction assay. The measurement was carried out in 1 ml cuvettes, which were incubated at appropriate temperatures. Each bar represents the mean and standard deviation of three independent measurements.

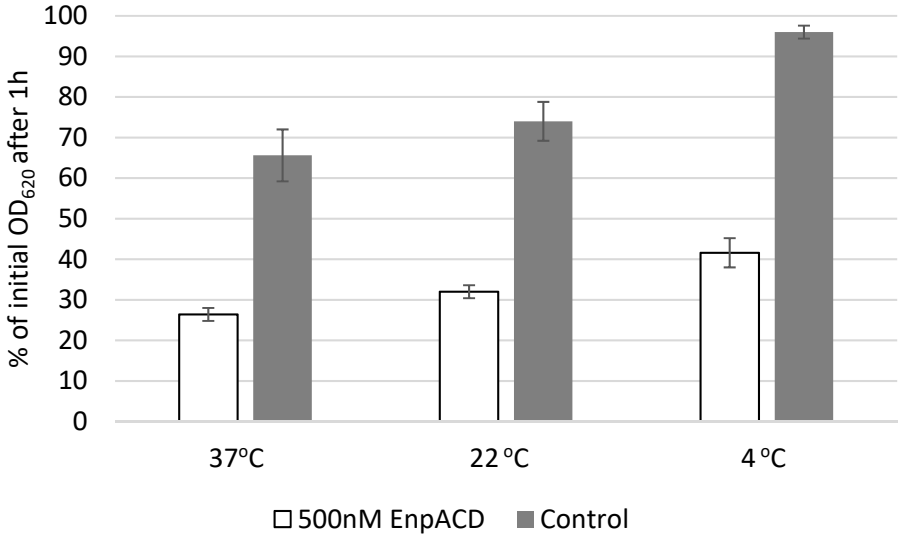

Figure S6. The effects of modifications of *S. aureus* cell wall on $EnpA_{CD}$ bacteriolytic activity. Results of the lytic test carried out on *S. aureus 8325-4* in glycine buffer pH = 8.0 for 1 hour. The final concentration of $EnpA_{CD}$ was 500nM, while LytM and Lss - 100nM. Each experiment was repeated three times using an enzyme from the same preparation and different bacterial cultures. Three technical repetitions were prepared each time. **(A)** The effect of the cross-bridge length. **(B)** The effect of serine substitution in cross-bridge. **(C)** The effect of presence of wall teichoic acids. Tests were run on various strains with synthesis of teichoic acids inhibited either by mutation in *tagO* gene or treatment with tunicamycin. The decrease in OD_{620} after one hour was calculated as a percentage of the initial OD_{620} in the control without the enzyme. The decrease in OD_{620}, in the control means autolysis, while in the sample the decrease in OD_{620} is due to autolysis and enzyme activity.

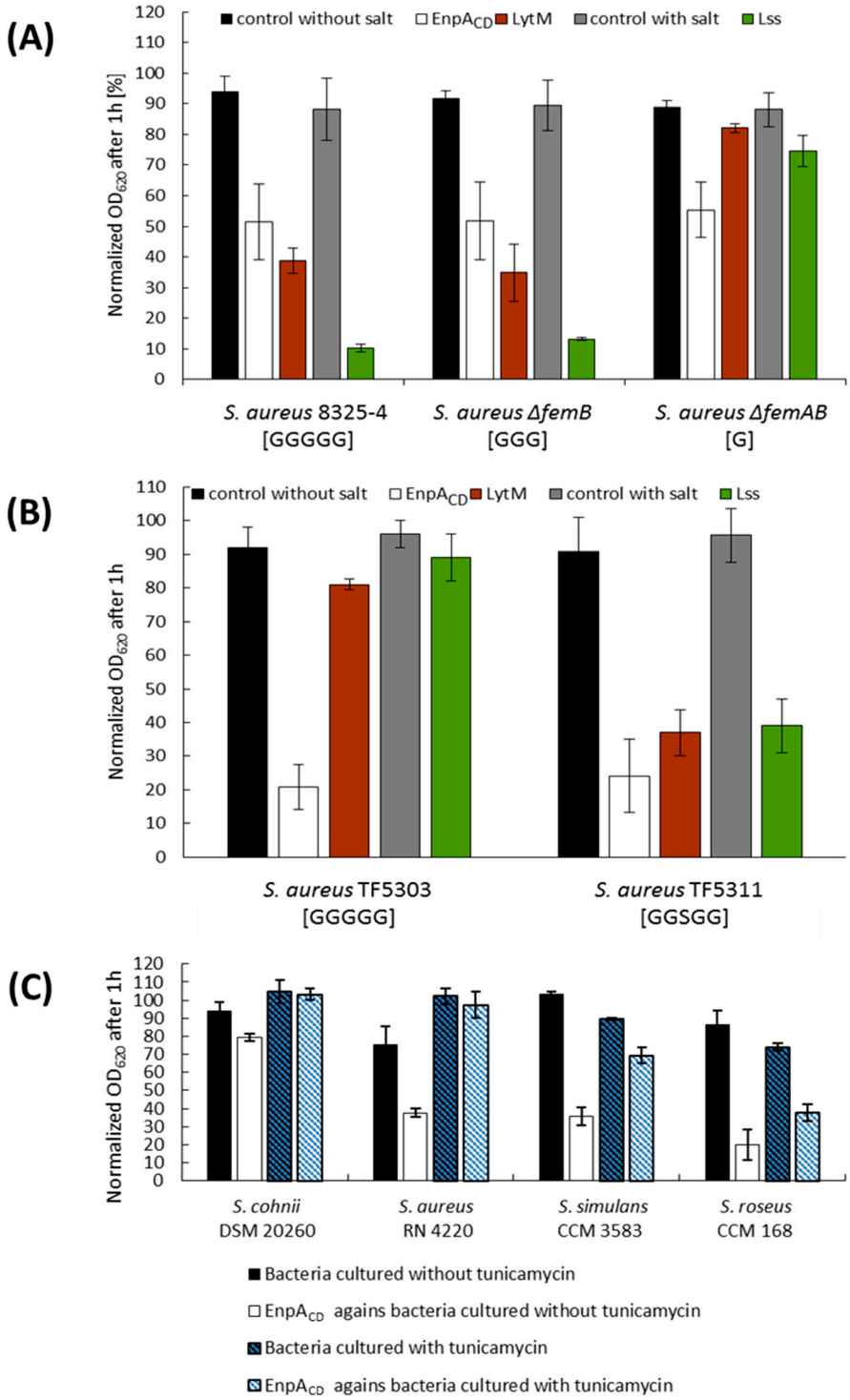

Figure S7. Structure of EnpA (pdb ID: 6SMK) and LysK CHAP domain (pdb ID: 4CSH)

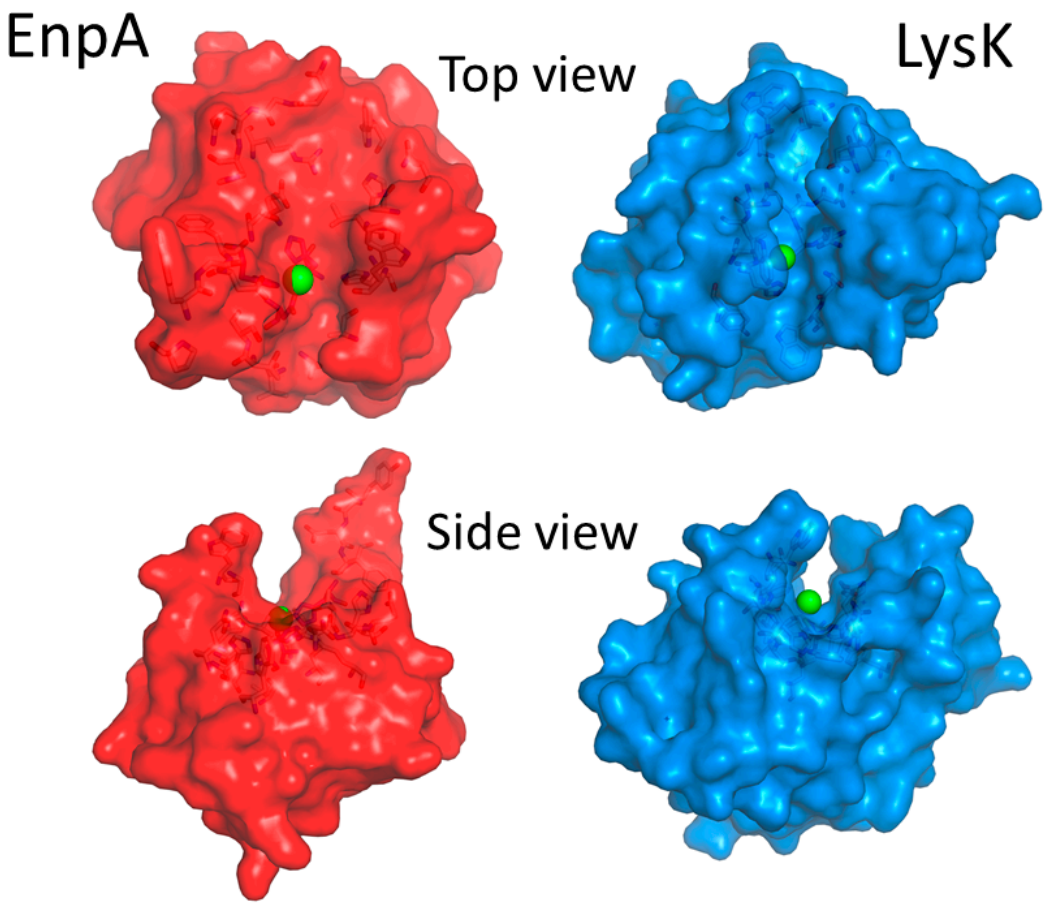

Figure S8. Amino acid sequence alignment of M23 enzymes based on structural and sequential constraints done using PROMSAL3D software[67] **.** The loop position is marked by blue rectangles and labeled. Zinc ligands in HxxxD and HxH motis are colored green. Conserved histidine residues taking part in catalysis are colored orange. Arg21 and its structural equivalents are colored red.

```
                                  21          29  33
>EnpA   PHFGS---PFVRTSDYG--KRPGLY--GDFHTGIDYAAP------TGTPIPAQYPGLVDWVQS------SSIGLG
>LytM   DASWL--TSRKQLQPYG--QYHGG----GAHYGVDYAMP------ENSPVYSLTDGTVVQAGW------SNYGGG
>Lss    SAQWL--NNYKKGYGYG---PYPLGINGGMHYGVDFFMN------IGTPVKAISSGKIVEAGW------SNYGGG
>Csd3   ETPV---KYTRISSPFSYGRFPVLKV-RRPHYGVDYAAK------HGSLIHSASDGRVGFMGV-------KAGYG
>Gp13   QFPM---DIINISQGE---NGSFS---HKGTLCIDFVGKT-----EKYPYYAPCDCTCVWRGD----------AS
>ZooA   GSATY---TRPLDTGNITTGFNGY----PGHVGVDYAVP------VGTPVRAVANGTVKFAGNGANHPWMLWMAG
>LasA   QLPWRQGYSWQPNGAHSN-----TGS-GYPYSSFDASYDWPRWGSATYSVVAAHAGTVRVLSR------------
>LytU   -------RGSRITETFG--KYQH-SPFDGKHYGIDFALP------KGTPIKAPTNGKVTRIFN-------NELGG
```

Loop 1

Loop 2

```
                                    78                                      109 111
>EnpA   EHVGIKVAD----------NLWAMYGHMSRIR--AKMGDKVKAGQIVGDVG----SSG----WSTGPHVHYELRK
>LytM   NQVTIKEANS---------NNYQWYMHNNRLT--VSAGDKVKAGDQIAYSG----STG----NSTAPHVHFQRMS
>Lss    NQIGLIENDG---------VHRQWYMHLSKYN--VKVGDYVKAGQIIGWSG----STG----YSTAPHLHFQRMV
>Csd3   KVVEIHLN-----------ELRLVYAHMSAFANGLKKGSFVKKGQIIGRVG----STG----LSTGPHLHFGVYK
>Gp13   AYLAWTSDKEVMCADGSVRYITWVNVHESPLP--FDVGKKLKKGDLMGHTGIGGNVTG-------GDHWHFNVID
>ZooA   NAVLIQHAD----------GMHTGYAHLSKIS--VSTDSTVKQGQIIGYTG----ATG----QVTGPHLHFEMLP
>LasA   CQVRVTHPS----------GWATNYYHMDQIQ--VSNGQQVSADTKLGVYAGNINTALCEGGSSTGPHLHFSLLY
>LytU   KVLQIAEDNG---------EYHQWYLHLDKYN--VKVGDRVKAGDIIAYSG----NTG---IQTTGAHLHFQRMK
```

Loop 3

```
>EnpA   GGP------------NGQHVNPD-TYGG------------
>LytM   GGIG-----------NQYAVDPT-SYLQSR----------
>Lss    NSFS-----------NSTAQDPM-PFLKS-----------
>Csd3   NS---------------RPINPL-GY--------------
>Gp13   GKEYQGWTKKPDSCLAGTELHIY-DVFAV----NNVEIIN
>ZooA   ANPN---WQN----GFSGRIDPT-GYIAN-----------
>LasA   NG---------------AFVSLQGASFGPYRINVGTSNYD
>LytU   GGVG-----------NAYAEDPK-PFIDQ---LPDG----
```

Loop 4

Figure S9. To evaluate the role of arginine R21 in $EnpA_{CD}$ activity we have generated a protein with substitution R21Y which showed no activity against tested bacterial strains (A). FTIR confirmed that introduced substitution does not have a negative effect on protein folding as the overall structure is preserved (B).

(A) Activity of $EnpA_{CD}$R21Y variant.

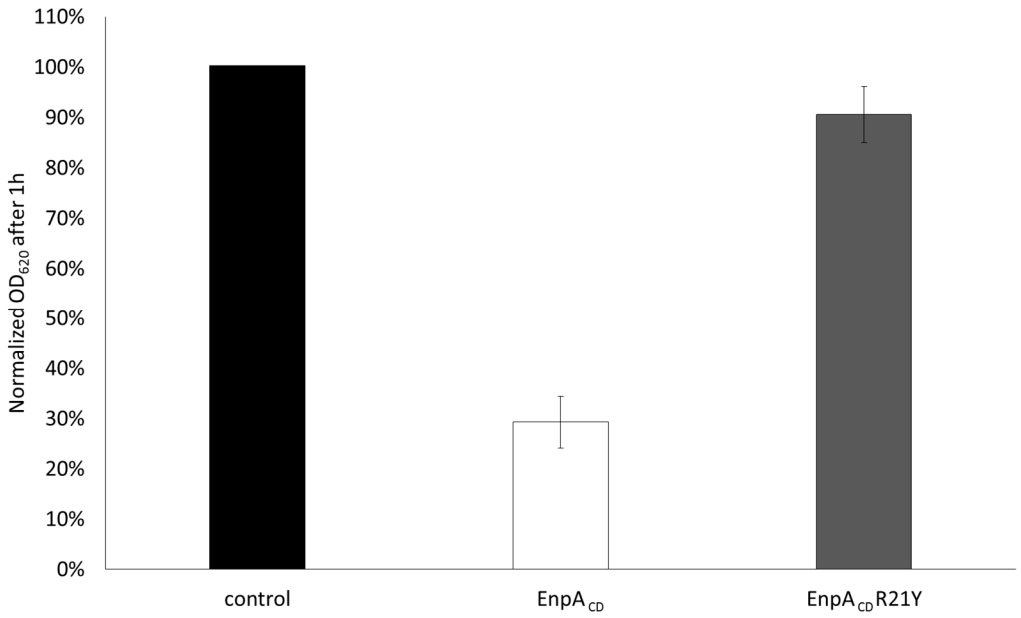
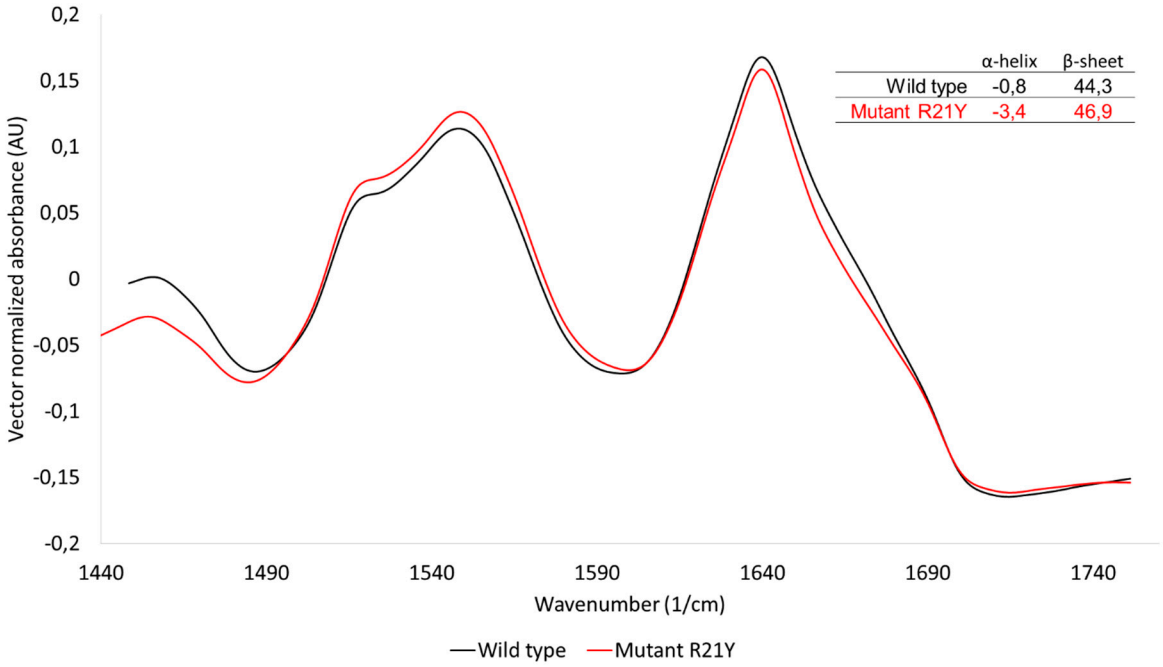
(B) Results of FTIR measurement. The graph shows the normalized absorbance for wild-type $EnpA_{CD}$ and the R21Y variant. The table shows the percentage of secondary structures in a particular protein.